Molecular Crystals and Liquid Crystals Incorporating Nonlinear Optics

Publication details, including instructions for authors and subscription information:
http://www.tandfonline.com/loi/gmcl17

Electrohydrodynamic Instability in Homeotropically Oriented Nematic Cyanobiphenyls

D. K. Rout [a] & R. N. P. Choudhary [a]

[a] Department of Physics and Meteorology, Indian Institute of Technology, Kharagpur, 721302, India

Version of record first published: 04 Oct 2006.

To cite this article: D. K. Rout & R. N. P. Choudhary (1989): Electrohydrodynamic Instability in Homeotropically Oriented Nematic Cyanobiphenyls, Molecular Crystals and Liquid Crystals Incorporating Nonlinear Optics, 172:1, 99-114

To link to this article: http://dx.doi.org/10.1080/00268948908042155

Mol. Cryst. Liq. Cryst., 1989, Vol. 172, pp. 99–114
Reprints available directly from the publisher
Photocopying permitted by license only

Printed in the United States of America

Electrohydrodynamic Instability in Homeotropically Oriented Nematic Cyanobiphenyls

D. K. ROUT and R. N. P. CHOUDHARY

Department of Physics and Meteorology, Indian Institute of Technology, Kharagpur 721302, India

(*Received September 13, 1988; in final form December 21, 1988*)

Electrohydrodynamic instability in a homeotropically oriented nematic phase of 8CB (4′-*n*-octyl-4-cyanobiphenyl), 8OCB (4′-*n*-octyloxy-4-cyanobiphenyl) and 9OCB (4′-*n*-nonyloxy-4-cyanobiphenyl) liquid crystals have been studied in an a.c. electric field. The domain patterns in these compounds in a low frequency a.c. field are very much similar to those in a d.c. field. The domain patterns observed at higher frequencies have been identified as "maltese crosses" or "crossed isogyres." The electroconvective "isotropic" flows near the electrode play an important role in the presently observed instability. The behavior of the threshold voltage with increasing frequency as well as temperature have been studied. The current density as a function of temperature, applied voltage and frequency of the applied field have also been studied. The charge injection from the electrode surface and the electrolytic process in the sample at low and high frequency a.c. field respectively are considered to be the basic mechanism responsible for the creation of a non-uniform charge distribution, which in-turn gives rise to the electroconvective flows.

1. INTRODUCTION

The occurrence of electrohydrodynamic (EHD) instability in the nematic liquid crystals having positive dielectric anisotropy ($\Delta\epsilon > 0$) is mainly falling under either of the two mechanisms: (a) Felici (Isotropic) mechanism occurring in an a.c. or d.c. electric field[1] or (b) Carr Helfrich mechanism.[2,3] A cellular/roll like domain pattern was first observed in homeotropically oriented 5CB (4′-*n*-pentyl-4-cyanobiphenyl)[4] and subsequently in 8CB[5,13] in d.c. electric field. This instability has been named as "Felici-Benard" type of instability (FBI) on account of its similarity to the Felici and Benard type of instability. The occurrence of FBI has largely been due to the charge injection from the electrode surface, convective fluid flow and the existence of the diffusion process.[4,5,13] It has further been shown[6,7] that the convective flows caused by the application of an a.c. field give rise to domain patterns in homeotropically oriented liquid crystals ($\Delta\epsilon > 0$). In a thin layer of nematic liquid crystal, the domains appear in the form of crossed isogyres or maltese crosses.[8] The convective flows producing these domains in the nematic phase have also been observed in the isotropic phase. That is why, this instability in low

frequency a.c. field has been termed as the "isotropic." The physical reason for this type of instability is a non-uniform field distribution near the electrodes,[9] which arises in the form of vortices near both the electrodes.

Although significant work on EHD instability in some nematic liquid crystals having $\Delta\epsilon >> 0$ has been reported in the recent past, numerous observed domain patterns often led to confusion. The instability modes in homeotropically oriented nematic liquid crystals in an a.c. electric field are not very clearly understood yet. Therefore, systematic studies of EHD instabilities in homeotropically oriented nematic cyanobiphenyls have been completed to provide a better understanding of the phenomena.

2. EXPERIMENTAL

The following compounds obtained from M/S BDH Ltd., U.K. were used without further purification. The reported transition temperatures[10] mentioned below along with the compounds while heating, have been confirmed in our studies.

(a) 8CB: 4′-*n*-octyl-4-cyanobiphenyl

K 21.5°C SmA 33.5°C N 40.5°C I

(b) 8OCB: 4′-*n*-octyloxy-4-cyanobiphenyl

K 55°C SmA 67°C N 80°C I

(c) 9OCB: 4′-*n*-nonyloxy-4-cyanobiphenyl

K 64°C SmA 77°C N 80°C I

Where, K, SmA, N, and I are the solid, smectic A, nematic and isotropic phases respectively.

For the application of an electric field to the samples, we used SnO_2 coated glass plates between which the samples are sandwiched. Mylar spacers of 50 and 75 μm thick were used to determine the sample thickness. Homeotropic alignment was obtained by pre-treating the glass plates with the standard methods. The temperature during the measurements were controlled with the help of an Indotherm temperature controller and a hot stage designed by us and described elsewhere.[5] The hot stage was mounted on a Censico polarizing microscope stage for visual observation and microphotographic work.

Ac voltage (0–20 Volts rms) was applied to the sample cell using a function generator (HIL 2821) in the frequency range 0.1 Hz to 20 kHz. The current flow-through the sample was measured by the voltage drop across a resistance connected in series. The rms voltage of the function generator was measured with the help of an a.c. microvoltmeter (systronics, type 411).

3. MICROSCOPIC OBSERVATIONS

From the microscopic examination, initial homeotropic alignment was found to be very good. Figure 1, shows the domain patterns of 8OCB at 5 volts a.c. (20 Hz, square wave). The domain pattern (elongated quadrants of the crossed isogyres/ maltese crosses) is similar to those observed in a d.c. field. Figures 2(*a*–*h*) show the domain patterns of 8OCB at various applied voltages at a frequency of 0.2 kHz (square wave). It has been observed that the maltese crosses begin to appear at 6.5 V for this frequency. All the four quadrants belong to a single maltese cross are not visible everywhere. On increasing the voltage, maltese crosses appear fully and become symmetrical (at 8.0 Volts) (Figure 2*c*). It has been noted that the elongated quadrants begin to shrink with increasing applied field and maltese crosses become more prominent (Figures 2*d*, *e*). At 11 volts (Figure 2*f*) a partial dissipation of the domain pattern starts, as a result of which the domain patterns become irregular (i.e. the quadrants of maltese crosses move away from each other). With subsequent application of higher voltage, fluid flow in the plane of the glass plates is clearly observed and hence, the regular maltese crosses are no longer visible (Figures 2*g*, *h*).

The domain patterns described above have also been observed in the other two compounds, except for some small changes in the threshold voltage, V_{th}. Some general features of the domain patterns of the above compounds observed in an a.c. field are as follows:

a) The domain patterns at very low frequencies (<10 Hz) are similar to those observed in a d.c. field.[4,5,13] The appearance of the domain pattern has a threshold character. The threshold varies with the compounds, quality of the initial homeotropic alignment and electrical conductivity of the sample.

b) At higher frequencies (>10 Hz), the elongated domain patterns gradually diminish and only maltese crosses are visible.

c) At a high (>0.5 k V^{-1} cm) electric field, the fluid flow is clearly visible, which destabilizes the domain patterns leading to a partial fluctuation of the pattern but no dynamic scattering was observed.

(d) The instability appears in the form of vortex flows localized in narrow layers near the electrodes. The fluid flow persists even in the isotropic liquid state. The

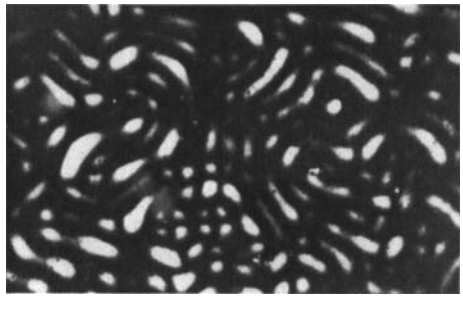

FIGURE 1 Domain patterns in 8 OCB at 5V 20 Hz square wave frequency.

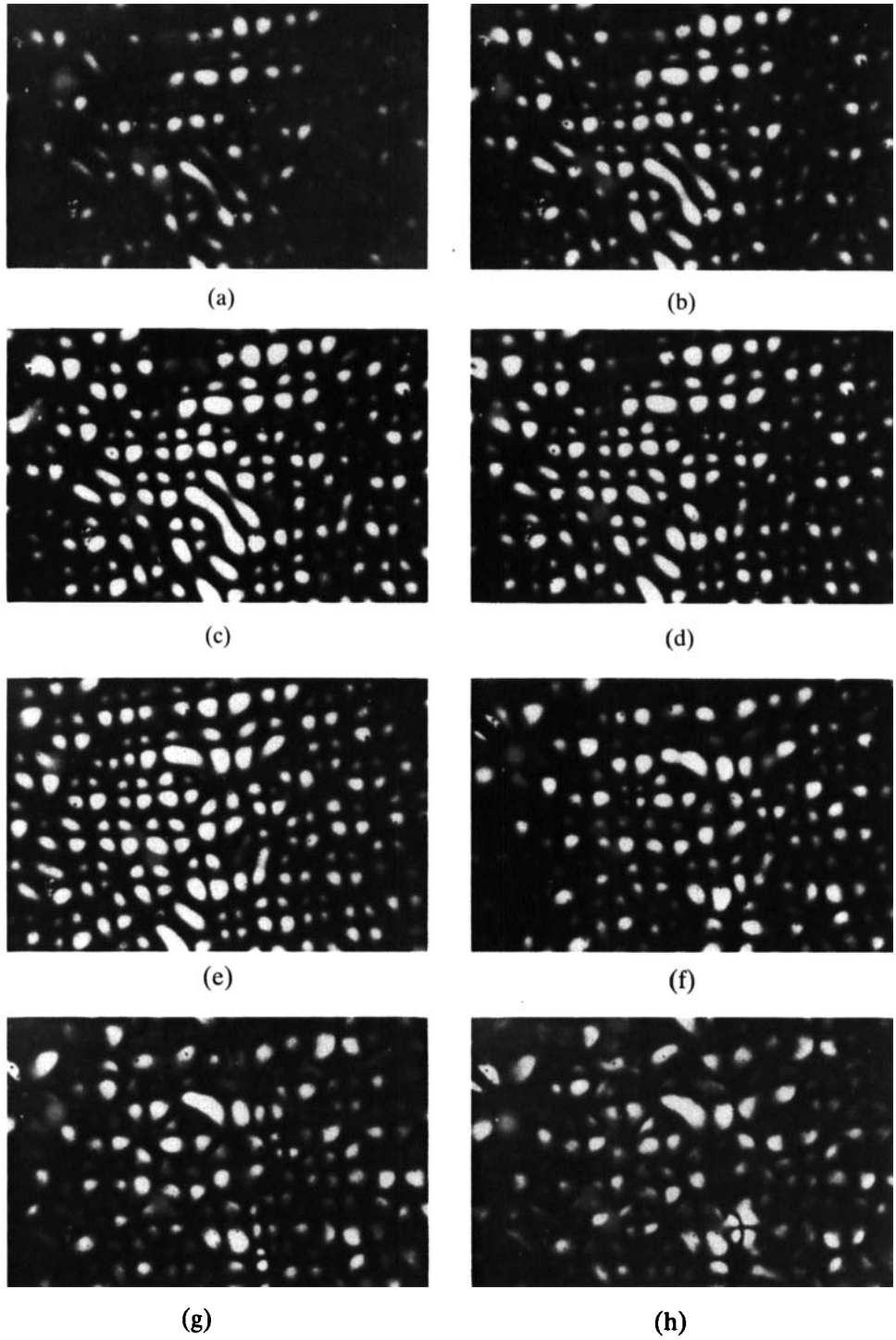

FIGURE 2 Domain patterns in 8 OCB at 0.2 kHz square wave frequency (a) 6.5 V (b) 7 V (c) 8 V (d) 9 V (e) 10 V (f) 11 V (g) 15 V (h) 17 V.

threshold voltage for the vortex flow is equal to that of domain patterns. A circular flow of impurity particles are also observed in the liquid phase and the flow is perpendicular to the initial alignment of the molecules and in the plane of the glass plates.

(e) The non-uniformity in the appearance of the domain pattern may be due to the non-uniformity of the effective field on the sample. The appearance of domains takes place after a few seconds (10–15 sec) of the application of the electric field.

4. FREQUENCY–THRESHOLD VOLTAGE CHARACTERISTICS

During our observations, we noted that the onset of vortex flow[9] and the appearance of domain patterns take place almost at the same time. Figures 3(*a*–*c*) show the frequency–threshold voltage characteristics for 8CB, 8OCB and 9OCB respectively. Similar type of behavior was found for all three compounds except for a small variation in V_{th} and the frequency range for different instability modes. The general features of V_{th}—f characteristics are as follows: In the very low frequency region, V_{th} increases slowly with increasing field frequency until a plateau (in V_{th}) is observed. The width of the plateau is found to be different for different compounds. It has also been observed that the plateau will be more pronounced with

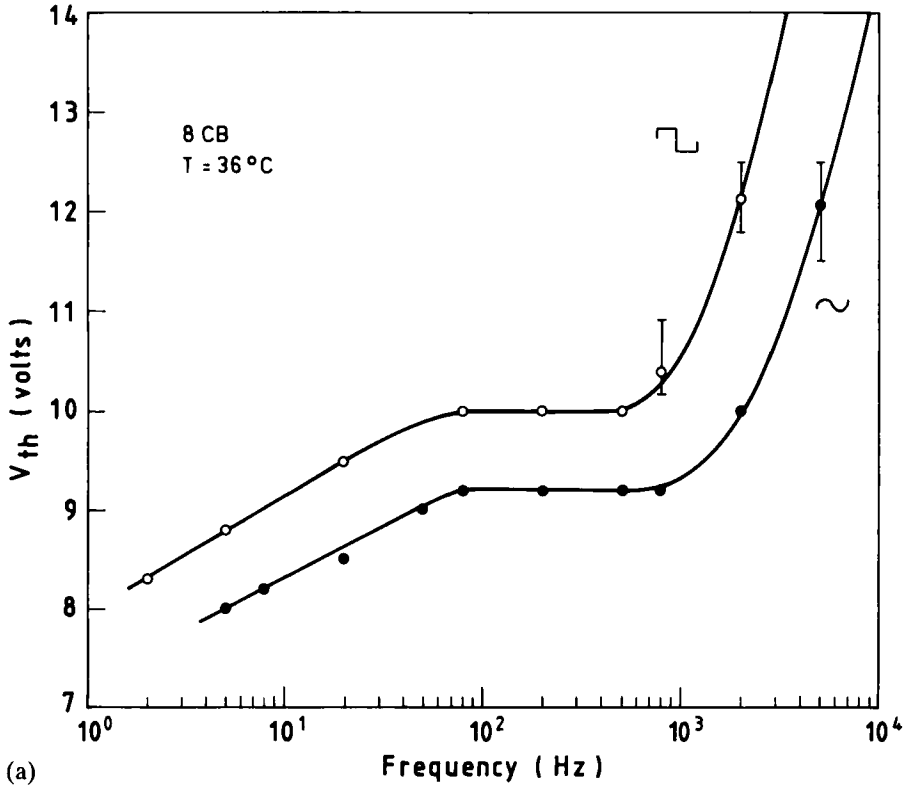

(a)

FIGURE 3 Frequency dependence of the threshold voltage (V_{th}) (a) 8 CB (b) 8 OCB (c) 9 OCB.

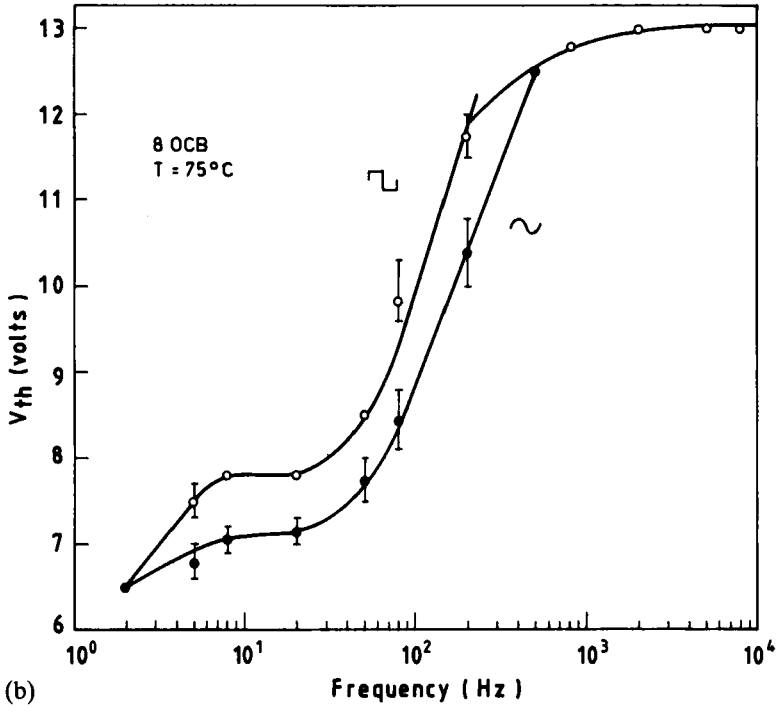

(b)

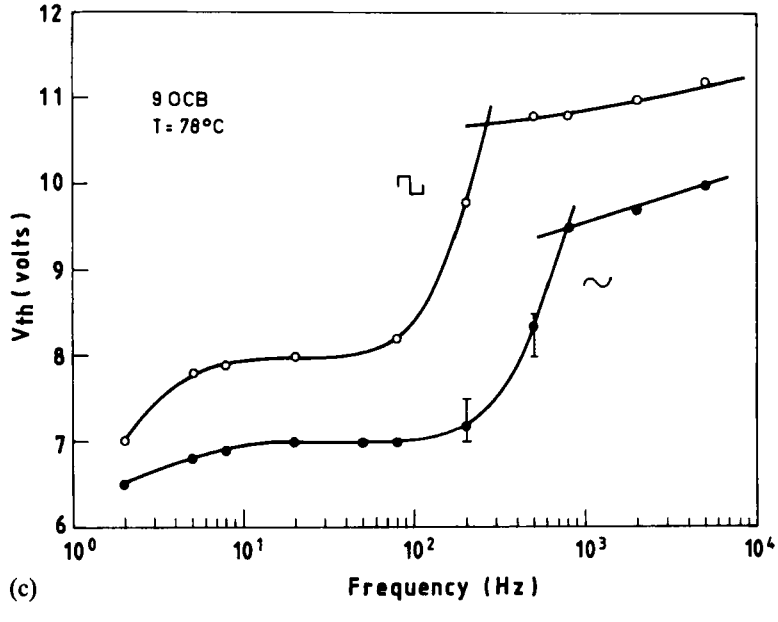

(c)

FIGURE 3 Continued

the aging of the sample, which can be seen in the case of 8CB. Beyond the plateau region, V_{th} increases steeply at a frequency, called the critical frequency, f_c, which also depends greatly on the aging of the sample. For a fresh sample, f_c is in the region of 10^2–10^3 Hz. For a squarewave excitation, f_c is lower than that of sine wave excitation as expected. Above f_c, the domain patterns are not very distinct and hence, values of V_{th} are not very accurate ($\pm 10\%$). Above f_c, V_{th} increases with the frequency rather slowly as is evident from the Figures 3(a–c). The conductivity values (σ_{11}) at the corresponding temperature at which measurements were taken are also given along with the figures.

As far as the authors know, the above type of $V_{th} - f$ characteristics have not been reported anywhere for homeotropically aligned nematic liquid crystals with $\Delta\epsilon > 0$. An attempt has been made to explain the observations. At very low frequencies (< 10 Hz), the instability is primarily due to the Felici injection mode, which normally occurs in a d.c. or low frequency a.c. field.[4,5] The charge injection from the electrode surface causes the space charge to build-up near the cathode and as a result of which convective flow occurs. This is analogous to the Benard's problem of thermal convection. For this reason, the instability under a d.c. field has been rightly termed as Felici-Benard instability.[4,5,13]

With increasing frequency of the applied field, the variation of the space charge along the x-coordinate (Figure 4) becomes out of phase with the external field. Thus the effective force exerted by the external field on the space charge decreases. Hence to create an instability, the external field has to be increased. However, with further increase in the applied frequency ($> f_c$), the charge injection from the electrode surface does not exist any more. The space charge formation seems to occur due to the electrolytic separation of positive and negative charges by the application of electric field itself. Near the electrode, the space charge gradient, δq_z, which is proportional to (γ.E), where γ is electrokinetic coefficient, coincides with the field direction (z – axis). The electric field produces a destabilizing force E.δq_z just again in the same way as a temperature gradient destabilizes a liquid placed in the gravity field (Benard problem).

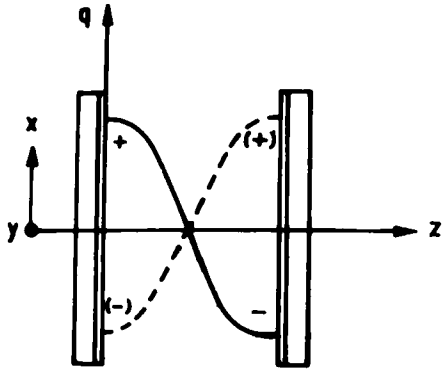

FIGURE 4 Schematic diagram of space charge distribution under an electric field.

Figure 5 shows the variation of V_{th} with the temperature of the mesophase. V_{th} decreases monotonically with the temperature in contrast to the observations of Blinov et al.,[14] where there is a small increase in V_{th} values at the N–I transition. The voltage at which the impurity particles present in the sample start moving in the isotropic state is almost equal to V_{th} in the nematic phase. The continuity in V_{th} across the N–I transition has been observed by us, and which is also reported by Blinov et al.[14]

The present instability occurs due to the electro-convective flows resulting from the non-uniform distribution of space charge. The creation of space charge is due to the charge injection or the electrolytic process depending upon the frequency of the applied voltage as discussed earlier.

5. CURRENT-DENSITY MEASUREMENTS

The electrical conductivity of the sample plays a major role in the onset of EHD instability in nematic liquid crystals. Current density, J, was measured at different voltages applied to the sample and also at different temperatures.

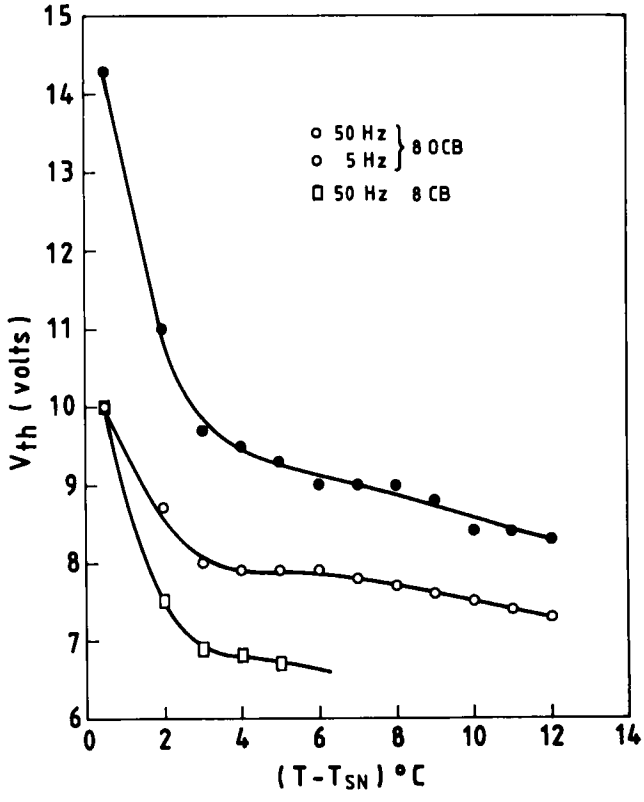

FIGURE 5 Variation of V_{th} with the temperature.

Figures 6(a–c) show the current density-voltage (J-V) characteristics of 8CB, 8OCB and 9OCB respectively. In all the cases, J increases linearly with increasing applied voltage at all the frequencies. For 8OCB and 9OCB, the values of current densities are higher than those for 8CB. This is because of the high temperature phase of the former compounds.

Figures 7(a–c) show the variation of current density with the frequency of the applied voltage (V_{th}) at different temperatures for 8CB, 80CB and 90CB respectively. With the increase of frequency, the electrical conductivity increases. This fact confirms the earlier assumption regarding the existence of the electrolytic process at higher frequencies. Further, at higher frequencies dispersion in the J values is also observed.

Figures 8(a–c) show the variation of the current density with the temperature at different frequencies. The values of J increase with the temperature. This observation is in contrast with that in a d.c. field, where there is a steep increase in J with temperature.

Considering the ionization-recombination model[12] in the case of a nematic liquid

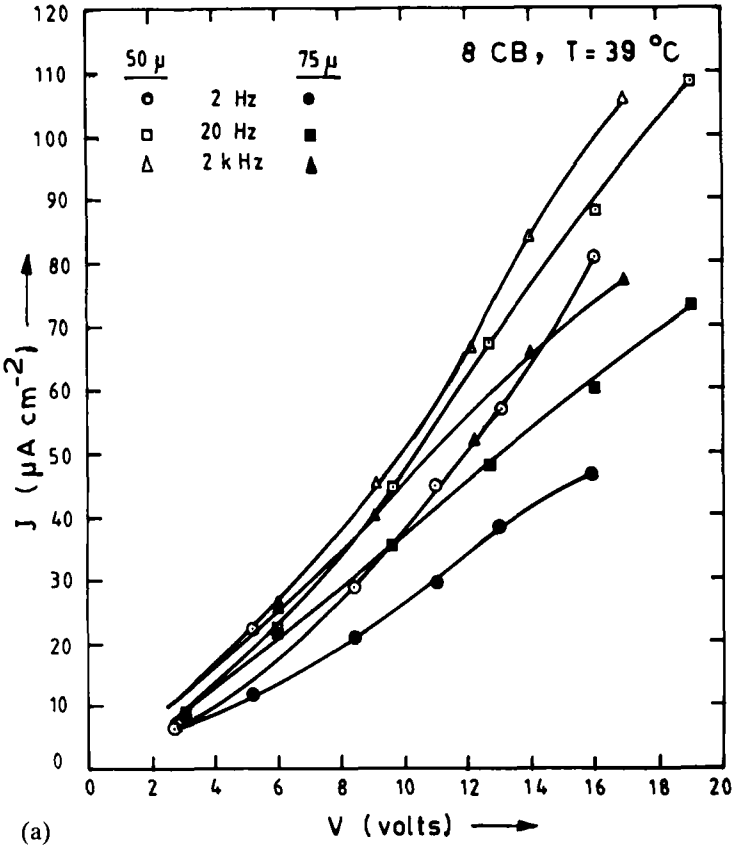

FIGURE 6 Current density—voltage characteristics (a) 8 CB (b) 8 OCB and (c) 9 OCB.

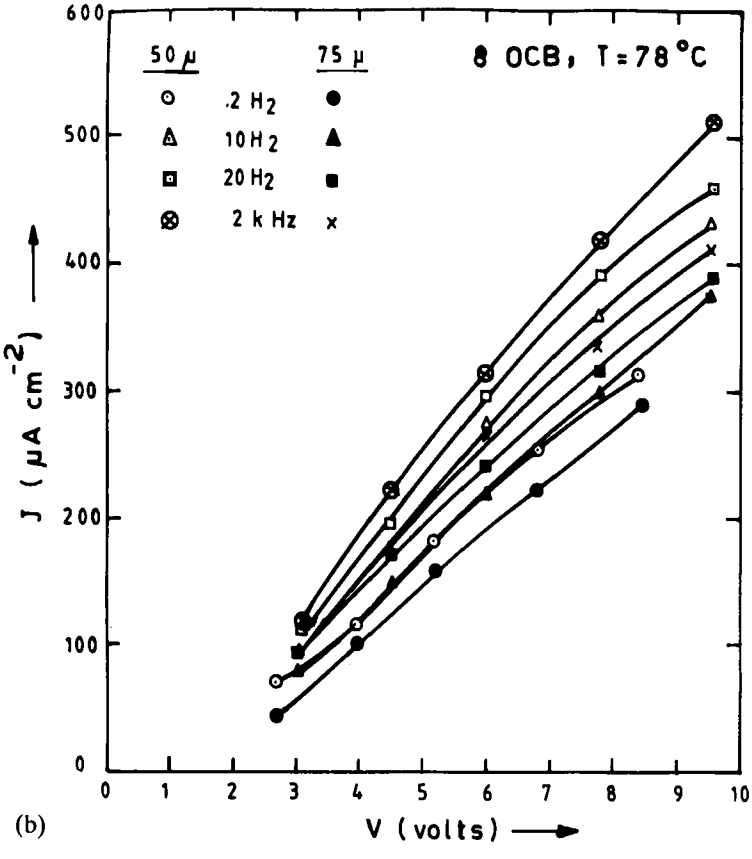

(b)

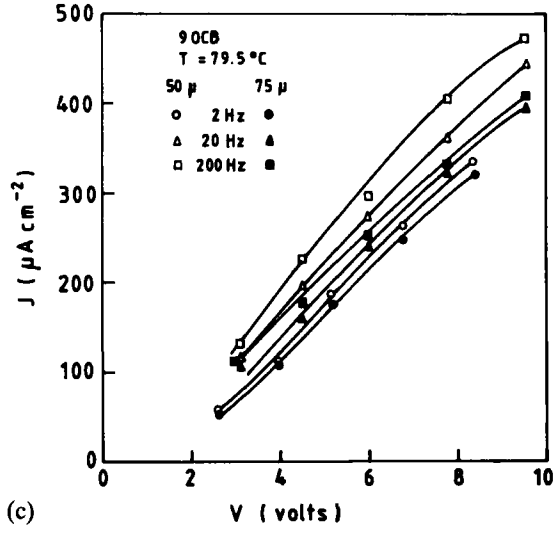

(c)

FIGURE 6 Continued

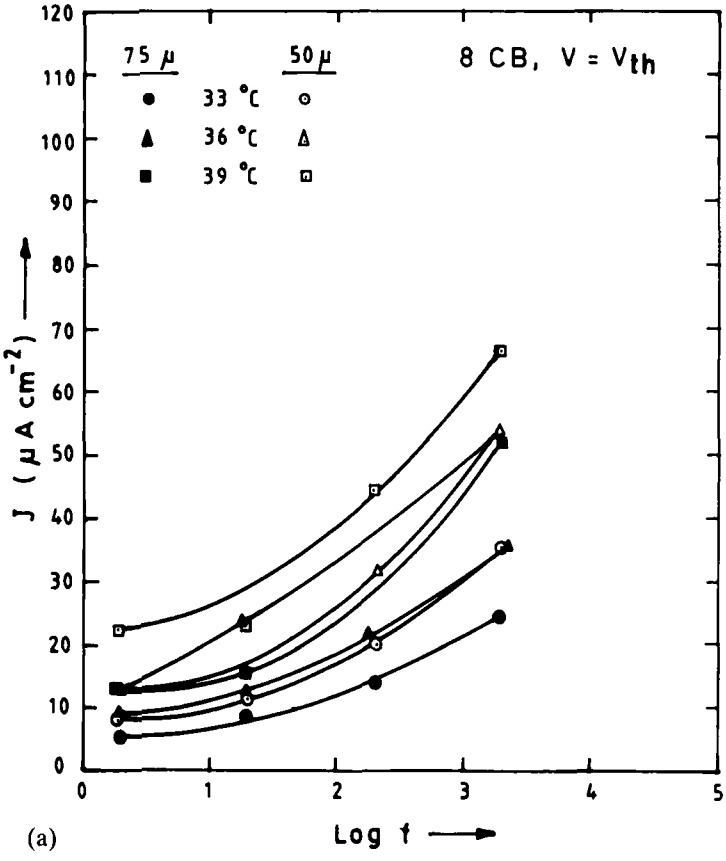

FIGURE 7 Frequency dependence of current density at different temperatures (at $V = V_{th}$) of (a) 8 CB (b) 8 OCB and (c) 9 OCB.

crystal in a d.c. or low frequency a.c. field, the ion concentration resulting in the conduction process can be given by the equation.

$$\frac{dn}{dt} = K_D C - K_R n^2 - \frac{E(\mu p + \mu n)}{d} - n \tag{1}$$

where d is the cell thickness, μp, μn are the mobilities of the positive and negative ions respectively; C is the concentration of the impurity per unit volume, E is the electric field and n_p, n_n are the positive and negative ion densities respectively ($n_p = n_n = n$). Heilmeier *et al.*[12] assumed that the direct recombination of ions is small enough to be neglected, and hence the current through the cell is given by

$$I \alpha Cd \exp \beta (-E/k_B T)^{1/2} \tag{2}$$

where β is a constant.[12]

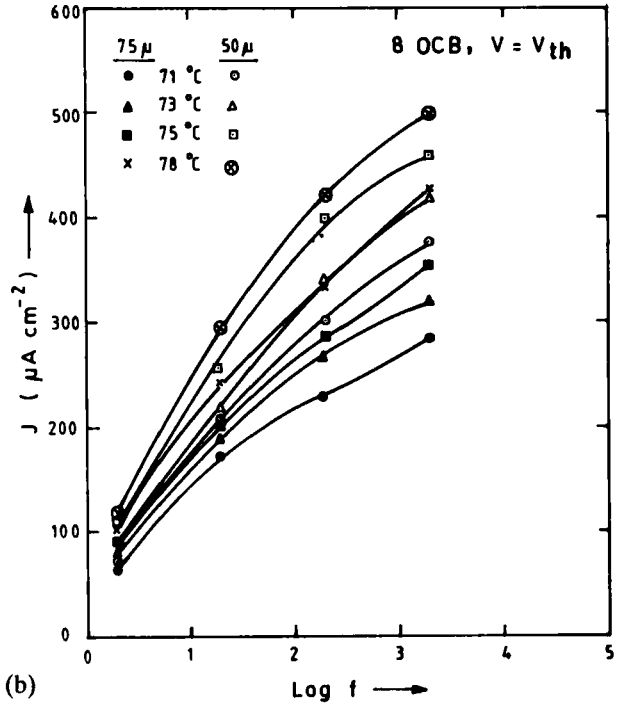

(b)

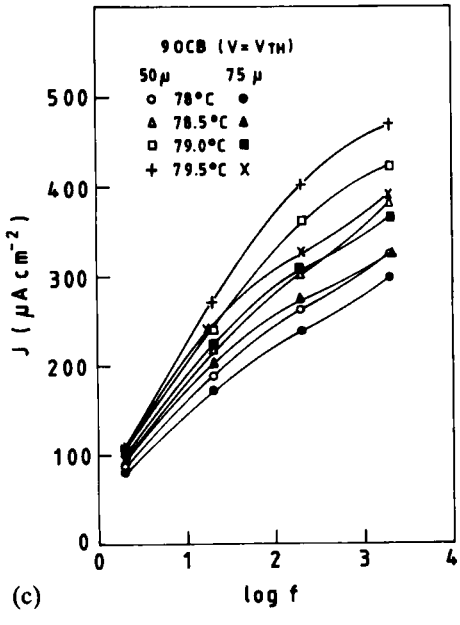

(c)

FIGURE 7 Continued

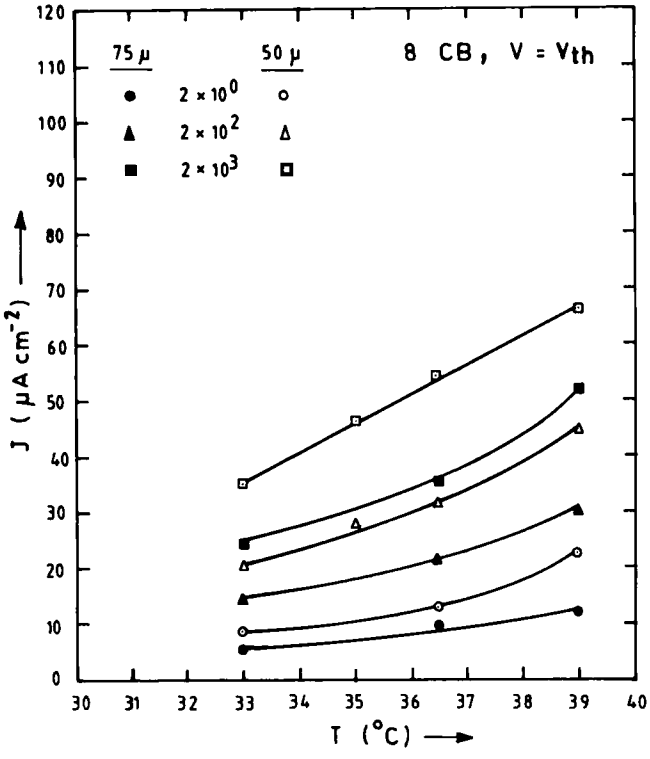

FIGURE 8 Temperature dependence of current density at different frequencies (at $V = V_{th}$) for (a) 8 CB, (b) 8 OCB, (c) 9 OCB.

According to Equation (2), the current density is strongly field dependent and also proportional to the cell thickness. In fact, in 8CB and 8OCB, higher current density is observed for a 75μ thick cell than that of a 50μ cell at a particular field.[13]

In an a.c. field (symmetric square wave), when the period of the external field ($\tau = \epsilon/4\pi\sigma$) is less than the transit time of the ions between the electrodes, the drift of the carriers to the electrodes can be neglected (otherwise, it is quite prominent in a d.c. field). Hence we get only a linear increase in the current values with the applied field, unlike behavior in a d.c. field.[5,13]

The current density shows saturation (Figures 7*b*, *c*) at higher frequencies (> 10^3 Hz) of the applied field. Although, at higher frequencies, the charge injection from the electrode is quite suppressed, the space charge gradient is maintained by the electrolytic process in a high frequency a.c. field. Since the current values are measured at V_{th} (slow increases of V_{th} around 10^3 Hz), the current density thus tend to saturate. There is a slight exception to this observation in the case of 8CB (Figure 7*a*). In fact, in the case of 8CB, f_c is found to be above 10^3 Hz. Hence the tendency to saturate in the current density has not yet been observed at about 10^3 Hz frequency.

Unlike in a d.c. field, the current density increases linearly with increasing temperature at all frequencies. At or above the threshold voltage of the d.c. instability,

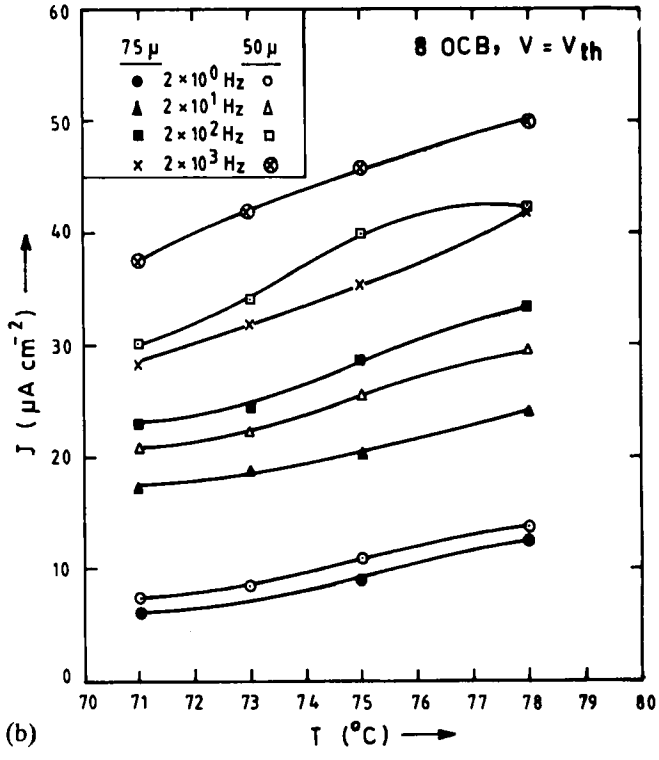

(b)

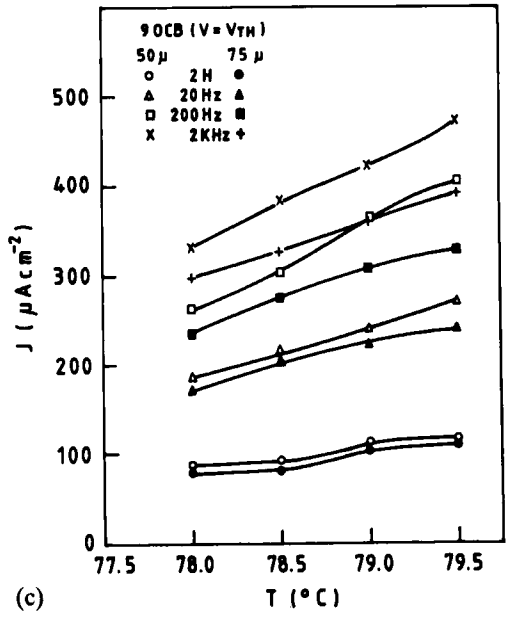

(c)

FIGURE 8 Continued

current values steeply increase with the rise in temperature. But at the threshold voltage of the a.c. instability, only a small temperature dependence is observed. The charge injection due to a thermonic emission process which is so prominent in a d.c. field is absent in the a.c. instability.

6. DISCUSSION AND CONCLUSION

In view of the present classification scheme of different modes of EHD instability,[8] the results in the present compounds can not be entirely classified. At very low frequencies (< 10 Hz), only a cellular domain pattern unlike the finger print pattern[6] was observed in the present case. The cellular domain pattern is a characteristic of the instability in a d.c. field. So the low frequency instability mode is explained as Felici injection mode. The plateau in V_{th}-f characteristics, to our knowledge, has not been reported so far in this type of electro-convective instability. The width of the plateau mainly depends upon the history of the sample. The isotropic high frequency (electrolytic mode) is present above f_c. However the accurate determination of V_{th} in the frequency region above f_c is difficult, since the domain patterns are not very distinct. This type of observation was also made by Gruler and Meier[11] in heptoxy-azobenzene. Hence the exact relation of V_{th}-f is not possible from the present data.

The non-uniform charge distribution caused either by the charge injection or by the electrolytic process is responsible for the vortex flow to occur. The flow has a critical velocity[14,15] at which the instability occurs. The vortex flows persist even in the isotropic phase confirming the isotropic nature of the instability.

Hysteresis in the J-V characteristics as observed in 5CB by Nakagawa and Akahane[4] was not found in the present compounds. The total current is contributed by the ohmic part and the convective part, whereas the current due to diffusion process is not present in an a.c. instability. The current density at the threshold voltage at various frequencies agrees well with the threshold voltage-frequency characteristics.

In summary, the instability in a homeotropically oriented nematic liquid crystal with $\Delta\epsilon >> 0$ in a stabilizing a.c. field is due to the electro-convective fluid flow caused by the non-uniform charge distribution in the sample.

Acknowledgements

The authors wish to acknowledge their gratefulness to M/s BDH Ltd., U.K. for providing the cyanobiphenyls used in the present study. DKR is grateful to the CSIR, New Delhi for a research fellowship. We also thank Prof. K. V. Rao and Dr. G. D. Nigam for their kind help and encouragement.

References

1. W. Pickard, Progress in Dielectrics, 6, 1 (1965).
2. E. F. Carr, *Adv. Chem. Ser.*, **63,** 86 (1967).
3. W. Helfrich, *J. Chem. Phys.*, **51,** 4092 (1969).
4. M. Nakagawa and T. Akahane, *J. Phys. Soc. J.*, **52,** 3773 (1983); ibid., **52,** 3782 (1983).

5. D. K. Rout and R. N. P. Choudhary, *Mol. Cryst. Liq. Cryst.*, **154,** 241 (1988).
6. M. I. Barnik, L. M. Blinov, M. F. Grebenkin and A. N. Trufanov, *Mol. Cryst. Liq. Cryst.*, **37,** 47 (1976).
7. M. I. Barnik, L. M. Blinov, S. A. Pikin and A. N. Trufanov, *Sov. Phys. JETP.*, **72,** 756 (1977).
8. L. M. Blinov, M. I. Barnik and A. N. Trufanov, *Mol. Cryst. Liq. Cryst.*, **89,** 47 (1982), L. M. Blinov, *Sci. Prog.*, **70,** 278, 263 (1986).
9. L. M. Blinov, M. I. Barnik, V. T. Lazareva and A. N. Trufanov, *J. Physique*, **40,** C3-236 (1979).
10. Data sheets supplied by M/s B.D.H. Ltd., U.K.
11. H. Gruler and G. Meier, *Mol. Cryst. Liq. Cryst.*, **12,** 289 (1971).
12. G. H. Heilmeier, L. A. Zanoni and L. A. Barton, *Proc. IEEE*, **56,** 1162 (1968).
13. D. K. Rout and R. N. P. Choudhary, Physics Teacher (to be published).
14. L. M. Blinov, A. N. Trufanov, V. G. Chigrinov and M. I. Barnik, *Mol. Cryst. Liq. Cryst.*, **74,** 1 (1981).
15. P. Manneville and E. Dubois-Violette, *J. Physique*, **37,** 285 and 1115 (1976).